Copyright © 2012 Tech Science Press CMC, vol.29, no.1, pp.41-74, 2012

Local Buckling Delamination of a Rectangular Sandwich Plate Containing Interface Embedded Rectangular Cracks and Made From Elastic and Viscoelastic Materials

S.D. Akbarov[1,2], **N. Yahnioglu**[1] **and A. Tekin**[1]

Abstract: A three-dimensional buckling delamination problem for a rectangular sandwich plate made from elastic and viscoelastic materials is studied. It is supposed that the plate contains interface embedded rectangular cracks and that the edge-surfaces of these cracks have initial infinitesimal imperfections. The evolution of these initial imperfections with an external bi-axial compressed force (for the case where the materials of the layers of the plate are elastic) or with duration of time (for the case where the materials of the layers of the plate are viscoelastic) is investigated. The corresponding boundary value problem is formulated within the framework of the piecewise homogeneous body model with the use of three-dimensional geometrically nonlinear field equations of the theory of viscoelastic bodies. This problem is solved by employing boundary form perturbation techniques, Laplace transform and FEM. According to the initial imperfection criterion, the values of the critical parameters are determined. Numerical results on the critical force and critical time are presented and discussed. In particular, it is established that the values of the critical forces obtained for the buckling delamination around the rectangular embedded interface cracks are significantly greater than those obtained for the corresponding edge and band cracks.

Keywords: Buckling delamination, sandwich plate, embedded interface crack, viscoelastic material, critical time, 3D FEM.

1 Introduction

Local buckling delamination of laminated composite materials is one of the common failure mechanisms in compression. This delamination takes place around the zones in which two adjacent layers are partially debonded at their interface. These debonded zones are formed as a consequence of various impact events, poor fabri-

[1] YTU, Istanbul, Turkey
[2] Inst. Math. Mech. of National Academy of Science of Azerbaijan, Baku, Azerbaijan

cation process and fatigue and, as a result, they reduce several times the compressive strength of the structures fabricated from the composed materials. Note that in the related research the mentioned debonded zones are modeled as cracks and the regions bounded by the cracks and the laminate free surface are liable to buckle locally under compressive loads, thereby creating conditions conductive to delamination growth and consequent global failure of the structure. A review of these researches is detailed in recent papers by Akbarov, Yahnioglu and Karatas (2010) and Akbarov, Yahnioglu and Tekin (2010). Nevertheless, here we reconsider a brief review, all of which are made within the scope of the Three-Dimensional Linearized Theory of Stability (TDLTS) of deformable solid body mechanics. Guz and Nazarenko (1985a, 1985b) made the first attempts in this field. Note that a detailed description of the field equations and relations of the TDLTS are given in many references, for instance in the monograph by Guz (1999) and a detailed description of some early results is given in other monographs by Guz (2008a, 2008b). The present level of these investigations is detailed in a paper of Bogdanov, Guz and Nazarenko (2009). However, in all these investigations it was assumed that the materials of the composites are time independent. Development of the TDLTS based on the initial imperfection stability loss criterion by Hoff (1954) for time dependent materials was proposed and employed in papers by Akbarov (1998, 2007), Akbarov, Sisman and Yahnioglu (1997), Akbarov and Yahnioglu (2001) and others. Consideration of some related results is also given in the monograph by Akbarov and Guz (2000). Development and application of the aforementioned version of the TDLTS on the study of the buckling delamination problems of the plate-strip and circular disc type elements of constructions fabricated from viscoelastic materials were made in the papers by Akbarov and Rzayev (2002a, 2002b, 2003), Rzayev and Akbarov (2002), Rzayev (2002) and others. A systematic review of these studies was considered in the survey paper by Akbarov (2007). However, in these studies, the two-dimensional (with respect to the space coordinates) problems were analyzed for a plate-strip containing a crack whose edges are parallel to the face planes of the plate and a circular plate containing a penny-shaped crack, the edge faces of which are also parallel to the plate's upper and lower face planes. Furthermore, these investigations were carried out by utilizing 2D FEM modeling. In papers by Akbarov and Yahnioglu (2010) and Akbarov, Yahnioglu and Karatas (2010) an attempt is made to develop the approach proposed in other papers by Akbarov and Rzayev (2002a, 2002b, 2003) for the three-dimensional buckling delamination problems for an anisotropic (transversal-isotropic) viscoelastic rectangular plate containing a band (Akbarov and Yahnioglu (2010)) and also for a rectangular edge crack under uniaxial compression (Akbarov, Yahnioglu and Karatas (2010)). Moreover, in a paper by Akbarov, Yahnioglu and Tekin (2010) this development was extended for a rectangular sandwich plate containing an interface band and

edge cracks. However, up to now there has not been any investigation on buckling delamination around the embedded cracks. Therefore, in the present paper the local buckling delamination problem for a sandwich plate containing two symmetric (with respect to the middle plane of the core layer of the plate) embedded interface rectangular cracks is studied under bi-axial compression. In other words, in the present work the investigation carried out in a paper by Akbarov, Yahnioglu and Tekin (2010) is developed for the sandwich plate containing two rectangular embedded cracks under bi-axial compression.

2 Formulation of the problem

Consider a thick rectangular sandwich plate, which contains two interface rectangular embedded cracks. The geometry of the plate and cracks are shown in Fig. 1a. The Cartesian coordinate system $Ox_1x_2x_3$ is associated with the plate so as to give Lagrange coordinates of the points on the plate in the natural state. Assume that the plate occupies the region $V = V^{(r_1)} \cup V^{(r_2)} \cup V^{(r_3)}$ where:

$$V^{(r_1)} = \{0 \le x_1 \le \ell_1;\ 0 \le x_2 \le h_F;\ 0 \le x_3 \le \ell_3\},$$
$$V^{(r_2)} = \{0 \le x_1 \le \ell_1;\ h_F \le x_2 \le h_F + h_C;\ 0 \le x_3 \le \ell_3\},$$
$$V^{(r_3)} = \{0 \le x_1 \le \ell_1;\ h_F + h_C \le x_2 \le h;\ 0 \le x_3 \le \ell_3\}. \tag{1}$$

We suppose that the plate contains two embedded rectangular interface cracks, one of which is at:

$$\Omega_1 = \{(\ell_1 - \ell_{10})/2 \le x_1 \le (\ell_1 + \ell_{10})/2;\ x_2 = h_F;\ (\ell_3 - \ell_{30})/2 \le x_3 \le (\ell_3 + \ell_{30})/2\}, \tag{2}$$

and the other one is at:

$$\Omega_2 = \{(\ell_1 - \ell_{10})/2 \le x_1 \le (\ell_1 + \ell_{10})/2; \quad x_2 = h_F + h_C;\ (\ell_3 - \ell_{30})/2 \le x_3 \le (\ell_3 + \ell_{30})/2\}. \tag{3}$$

In Eqs. (2) and (3) ℓ_{10} (ℓ_{30}) is the length of the crack along the axis Ox_1(Ox_3). It is assumed that the edge surfaces of the cracks have an insignificant initial imperfection and this imperfection is symmetric with respect to the interface planes and with respect to the $x_1 = \ell_1/2$ and $x_3 = \ell_3/2$ planes. The equations of the edge surfaces of the lower and upper cracks can be written as follows:

$$x_2^{\pm} = h_F + \varepsilon f^{\pm}(x_1, x_3), \quad x_2^{\pm} = h_F + h_C + \varepsilon f^{\pm}(x_1, x_3),$$

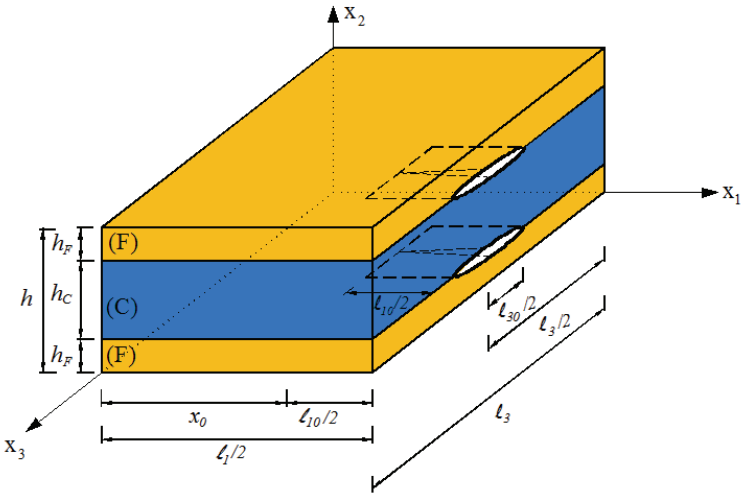

(a)

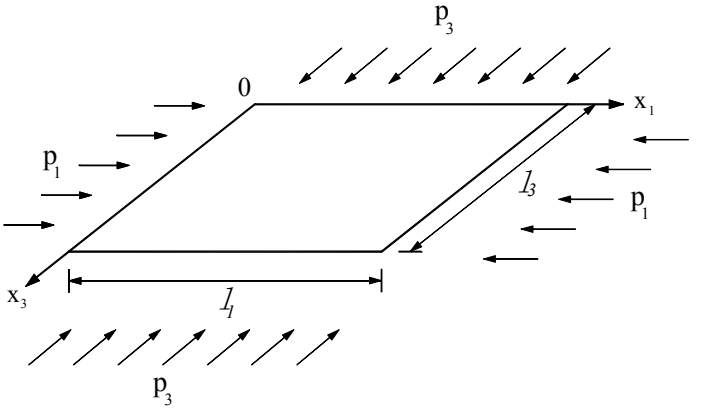

(b)

Figure 1: The geometry of the sandwich plate and interface rectangular embedded cracks

$$(\ell_1-\ell_{10})/2 \le x_1 \le (\ell_1+\ell_{10})/2, \quad (\ell_3-\ell_{30})/2 \le x_3 \le (\ell_3+\ell_{30})/2 \tag{4}$$

where ε is the dimensionless small parameter ($\varepsilon << 1$) which characterizes the degree of the initial imperfection of the crack edge-surfaces, h_F (h_C) is the thickness of each face layer (core layer) and the upper index "+" ("−") represents the upper (the lower) surface of the considered cracks. The function $f(x_1,x_3)$ satisfies the

following relations:

$$f^{+}(x_1,x_3) = -f^{-}(x_1,x_3),$$

$$f^{\pm}\left((\ell_1-\ell_{10})/2,x_3\right)\Big|_{(\ell_3-\ell_{30})/2\le x_3\le(\ell_3+\ell_{30})/2} = f^{\pm}\left((\ell_1+\ell_{10})/2,x_3\right)\Big|_{(\ell_3-\ell_{30})/2\le x_3\le(\ell_3+\ell_{30})/2} = 0,$$

$$\frac{\partial f^{\pm}\left((\ell_1-\ell_{10})/2,x_3\right)}{\partial x_1}\Bigg|_{(\ell_3-\ell_{30})/2\le x_3\le(\ell_3+\ell_{30})/2} = \frac{\partial f^{\pm}\left((\ell_1+\ell_{10})/2,x_3\right)}{\partial x_1}\Bigg|_{(\ell_3-\ell_{30})/2\le x_3\le(\ell_3+\ell_{30})/2} = 0,$$

$$f^{\pm}\left(x_1,(\ell_3-\ell_{30})/2\right)\Big|_{(\ell_1-\ell_{10})/2\le x_1\le(\ell_1+\ell_{10})/2} = f^{\pm}\left(x_1,(\ell_3+\ell_{30})/2\right)\Big|_{(\ell_1-\ell_{10})/2\le x_1\le(\ell_1+\ell_{10})/2} = 0,$$

$$\frac{\partial f^{\pm}\left(x_1,(\ell_3-\ell_{30})/2\right)}{\partial x_3}\Bigg|_{(\ell_1-\ell_{10})/2\le x_1\le(\ell_1+\ell_{10})/2} = \frac{\partial f^{\pm}\left(x_1,(\ell_3+\ell_{30})/2\right)}{\partial x_3}\Bigg|_{(\ell_1-\ell_{10})/2\le x_1\le(\ell_1+\ell_{10})/2} = 0. \quad (5)$$

Thus, we investigate the evolution of the foregoing initial infinitesimal imperfections of the crack-edge surfaces under bi-axial compression of the plate along the Ox_1 and Ox_3 axes with uniformly distributed normal forces with intensity p_1 and p_3 (Fig. 1b) respectively (for the elastic plate) and as time elapses at fixed values of the external compression forces (for the viscoelastic plate). As in the paper by Akbarov, Yahnioglu and Tekin (2010), this evolution will be investigated by utilizing the three-dimensional geometrically nonlinear equations of the theory of viscoelasticity in the framework of the piecewise homogeneous body model.

Below, the values relating to the core layer and the face layers will be denoted by upper indices (1) and (2) respectively. At the same time, we will use upper index r_k $(k = 1,2,3)$ where r_1 and r_3 indicate the values related to the lower and upper layers, respectively, but r_2 indicates the values related to the core layer, so that $r_1 = r_3 = 2$, $r_2 = 1$. It is assumed that the face layers of the sandwich plate are made from the same materials and the structure of the plate is symmetric with respect to the middle plane of the core layer.

Within the framework of the three dimensional geometrically nonlinear equations of the theory of viscoelasticity the governing field equations are:

Equilibrium equation:

$$\frac{\partial}{\partial x_j}\left[\sigma_{jn}^{(r_k)}\left(\delta_i^n+\frac{\partial u_i^{(r_k)}}{\partial x_n}\right)\right]=0,\quad i;j;n;k=1,2,3,\quad r_1=r_3=2,\quad r_2=1 \tag{6}$$

Geometrical relation:

$$\varepsilon_{ij}^{(r_k)}=\frac{1}{2}\left(\frac{\partial u_i^{(r_k)}}{\partial x_j}+\frac{\partial u_j^{(r_k)}}{\partial x_i}+\frac{\partial u_n^{(r_k)}}{\partial x_i}\frac{\partial u_n^{(r_k)}}{\partial x_j}\right), \tag{7}$$

Constitutive relation:

$$\sigma_{ij}^{(r_k)}=\lambda^{*(r_k)}\theta^{(r_k)}\delta_i^j+2\mu^{*(r_k)}\varepsilon_{ij}^{(r_k)},\quad \theta^{(r_k)}=\varepsilon_{11}^{(r_k)}+\varepsilon_{22}^{(r_k)}+\varepsilon_{33}^{(r_k)}, \tag{8}$$

where $\lambda^{*(r_k)}$ and $\mu^{*(r_k)}$ are the following operators:

$$\begin{aligned}\lambda^{*(r_k)}\phi(t)&=\lambda_0^{(r_k)}\phi(t)+\int_0^t\lambda^{(r_k)}(t-\tau)\phi(\tau)d\tau,\\ \mu^{*(r_k)}\phi(t)&=\mu_0^{(r_k)}\phi(t)+\int_0^t\mu^{(r_k)}(t-\tau)\phi(\tau)d\tau.\end{aligned} \tag{9}$$

In equations (6)-(9) conventional notation is used. Consider formulation of the boundary and contact conditions.

Boundary conditions at the ends of the plate:

$$u_2^{(r_k)}\Big|_{x_1=0;\ell_1}=0,\quad u_2^{(r_k)}\Big|_{x_3=0;\ell_3}=0,\quad \left[\sigma_{1n}^{(r_k)}\left(\delta_1^n+\frac{\partial u_1^{(r_k)}}{\partial x_n}\right)\right]\Big|_{x_1=0;\ell_1}=p_1,$$

$$\left[\sigma_{1n}^{(r_k)}\left(\delta_3^n+\frac{\partial u_3^{(r_k)}}{\partial x_n}\right)\right]\Big|_{x_1=0;\ell_1}=0,\quad \left[\sigma_{3n}^{(r_k)}\left(\delta_1^n+\frac{\partial u_1^{(r_k)}}{\partial x_n}\right)\right]\Big|_{x_3=0;\ell_3}=0,$$

$$\left[\sigma_{3n}^{(r_k)}\left(\delta_3^n+\frac{\partial u_3^{(r_k)}}{\partial x_n}\right)\right]\Big|_{x_3=0;\ell_3}=p_3 \tag{10}$$

Boundary conditions on the free face planes of the plate:

$$\left[\sigma_{2n}^{(r_1)}\left(\delta_i^n+\frac{\partial u_i^{(r_1)}}{\partial x_n}\right)\right]\Big|_{x_2=0}=0,\quad \left[\sigma_{2n}^{(r_3)}\left(\delta_i^n+\frac{\partial u_i^{(r_3)}}{\partial x_n}\right)\right]\Big|_{x_2=h}=0. \tag{11}$$

Boundary conditions on the cracks' edge surfaces:

$$\left[\sigma_{jn}^{(r_1)}\left(\delta_i^n+\frac{\partial u_i^{(r_1)}}{\partial x_n}\right)\right]\Big|_{S_1^-} n_j^-=0,\quad \left[\sigma_{jn}^{(r_2)}\left(\delta_i^n+\frac{\partial u_i^{(r_2)}}{\partial x_n}\right)\right]\Big|_{S_1^+} n_j^+=0,$$

$$\left[\sigma_{jn}^{(r_3)}\left(\delta_i^n+\frac{\partial u_i^{(r_3)}}{\partial x_n}\right)\right]\Big|_{S_2^+} n_j^+=0,\quad \left[\sigma_{jn}^{(r_2)}\left(\delta_i^n+\frac{\partial u_i^{(r_2)}}{\partial x_n}\right)\right]\Big|_{S_2^-} n_j^-=0,$$

$$S_1^{\pm}=\{((\ell_1-\ell_{10})/2\le x_1\le(\ell_1+\ell_{10})/2),\quad x_2^{\pm}=h_F+\varepsilon f^{\pm}(x_1,x_3),$$

$$((\ell_3-\ell_{30})/2\le x_3\le(\ell_3+\ell_{30})/2)\},$$

$$S_2^{\pm}=\{((\ell_1-\ell_{10})/2\le x_1\le(\ell_1+\ell_{10})/2),\quad x_2^{\pm}=h_F+h_C+\varepsilon f^{\pm}(x_1,x_3),$$
$$((\ell_3-\ell_{30})/2\le x_3\le(\ell_3+\ell_{30})/2)\}. \tag{12}$$

Contact conditions between the layers of the plate:

$$u_i^{(r_1)}\Big|_{\wp_1^-}=u_i^{(r_2)}\Big|_{\wp_1^+},\quad u_i^{(r_3)}\Big|_{\wp_2^+}=u_i^{(r_2)}\Big|_{\wp_2^-},$$

$$\left[\sigma_{2n}^{(r_1)}\left(\delta_i^n+\frac{\partial u_i^{(r_1)}}{\partial x_n}\right)\right]\Big|_{\wp_1^-}=\left[\sigma_{2n}^{(r_2)}\left(\delta_i^n+\frac{\partial u_i^{(r_2)}}{\partial x_n}\right)\right]\Big|_{\wp_1^+},$$

$$\left[\sigma_{2n}^{(r_3)}\left(\delta_i^n+\frac{\partial u_i^{(r_3)}}{\partial x_n}\right)\right]\Big|_{\wp_2^+}=\left[\sigma_{2n}^{(r_2)}\left(\delta_i^n+\frac{\partial u_i^{(r_2)}}{\partial x_n}\right)\right]\Big|_{\wp_2^-},$$

$$\wp_1^{\pm} = \{0 \le x_1 \le \ell_1,\ 0 \le x_2 \le h_F \pm 0,\ 0 \le x_3 \le \ell_3\} -$$

$$\{(\ell_1 - \ell_{10})/2 \le x_1 \le (\ell_1 + \ell_{10})/2,\ x_2 = h_F \pm 0,\ (\ell_3 - \ell_{30})/2 \le x_3 \le (\ell_3 + \ell_{30})/2\},$$

$$\begin{aligned}\wp_2^{\pm} = {} & \{0 \le x_1 \le \ell_1,\ 0 \le x_2 \le h_F + h_C \pm 0,\ 0 \le x_3 \le \ell_3\} - \\ & \{(\ell_1 - \ell_{10})/2 \le x_1 \le (\ell_1 + \ell_{10})/2,\ x_2 = h_F + h_C \pm 0, \\ & \qquad (\ell_3 - \ell_{30})/2 \le x_3 \le (\ell_3 + \ell_{30})/2\} \end{aligned} \quad (13)$$

where n_j ($n_j^{\pm}$) in equation (12) are the orthonormal components of the unit normal vector of the considered surfaces (i.e. acting on the cracks' edge surfaces). The other notation used in Eqs. (10)-(13) is conventional.

Having thus completed the formulation of the considered problem, we now consider the method of solution.

3 Solution procedure

First, using the equations of the crack edge surfaces given in (4), from the equation $x_2^{\pm} = h_F + \varepsilon f^{\pm}(x_1, x_3)$ or $x_2^{\pm} = h_F + h_C + \varepsilon f^{\pm}(x_1, x_3)$ we derive the following expressions for $n_j^{\pm}$:

$$n_1^{\pm} = \frac{\pm\varepsilon \frac{\partial f^{\pm}(x_1,x_3)}{\partial x_1}}{\sqrt{1 + \varepsilon^2 \left(\frac{\partial f^{\pm}(x_1,x_3)}{\partial x_1}\right)^2 + \varepsilon^2 \left(\frac{\partial f^{\pm}(x_1,x_3)}{\partial x_3}\right)^2}},$$

$$n_2^{\pm} = \frac{\pm 1}{\sqrt{1 + \varepsilon^2 \left(\frac{\partial f^{\pm}(x_1,x_3)}{\partial x_1}\right)^2 + \varepsilon^2 \left(\frac{\partial f^{\pm}(x_1,x_3)}{\partial x_3}\right)^2}},$$

$$n_3^{\pm} = \frac{\pm\varepsilon \frac{\partial f^{\pm}(x_1,x_3)}{\partial x_3}}{\sqrt{1 + \varepsilon^2 \left(\frac{\partial f^{\pm}(x_1,x_3)}{\partial x_1}\right)^2 + \varepsilon^2 \left(\frac{\partial f^{\pm}(x_1,x_3)}{\partial x_3}\right)^2}}. \quad (14)$$

Note that the expression (14) occurs for the surfaces $S_1^{\pm}$ and $S_2^{\pm}$ (12) simultaneously.

Assume that $\varepsilon^2\left[\left(\frac{\partial f^{\pm}(x_1,x_3)}{\partial x_1}\right)^2+\left(\frac{\partial f^{\pm}(x_1,x_3)}{\partial x_3}\right)^2\right]<<1$ according to which, the expression (14) can be represented in series form in terms of the small parameterε:

$$n_1^{\pm}=\sum_{k=0}^{\infty}\varepsilon^{2k+1}n_{1k}^{\pm}(x_1,x_3),\ n_2^{\pm}=\pm 1+\sum_{k=1}^{\infty}\varepsilon^{2k}n_{2k}^{\pm}(x_1,x_3),\ n_3^{\pm}=\sum_{k=0}^{\infty}\varepsilon^{2k+1}n_{3k}^{\pm}(x_1,x_3). \tag{15}$$

In equation (15), the explicit expressions of the coefficients $n_{1k}^{\pm}(x_1,x_3)$, $n_{2k}^{\pm}(x_1,x_3)$ and $n_{3k}^{\pm}(x_1,x_3)$ are too long, so they are not given here. At the same time, these expressions can be easily obtained by employing the well known power series expansion of the expressions given in (15). As in the paper by Akbarov, Yahnioglu and Tekin (2010), the sought values are represented in series form in terms of ε as follows:

$$\left\{\sigma_{ij}^{(r_k)};\varepsilon_{ij}^{(r_k)};u_i^{(r_k)}\right\}=\sum_{q=0}^{\infty}\varepsilon^q\left\{\sigma_{ij}^{(r_k),q};\varepsilon_{ij}^{(r_k),q};u_i^{(r_k),q}\right\}. \tag{16}$$

After substituting equation (16) into equations (6)-(8) and comparing identical powers of ε, we obtain the corresponding closed system of equations to describe each approximation. Owing to the linearity of the mechanical relations in equations (8) and (9) and the conditions for displacements in equations (10) and (13), these relations and conditions will be satisfied for each approximation in Eq. (16), separately. The remaining relations obtained from equations (6)-(8) and (10)-(13) for every q-th approximation contains the values of all the previous approximations. At the same time, while satisfying the boundary conditions on the crack's edge surfaces, i.e. the conditions in equation (12), we employ the boundary form perturbation technique, according to which, the values of each approximation in Eq. (16) related to the core layer are expanded in series in the vicinity of (x_1,h_F+0,x_3) and (x_1,h_F+h_C-0,x_3). However, using the values of each approximation in Eq. (16) related to the upper face (lower face) layer in the vicinity (x_1,h_F+h_C+0,x_3) (in the vicinity (x_1,h_F-0,x_3)), and using the expression (15), the corresponding conditions on the crack edge surfaces are also obtained for the first and subsequent approximations.

It follows from the well-known mechanical considerations that for the comparatively rigid composites under determination of the zeroth approximation we can use the relation $\delta_i^n+\frac{\partial u_i^{(0)}}{\partial x_n}\approx\delta_i^n$ according to which the field equations, boundary and contact conditions obtained from Eqs. (6)-(13) for the zeroth approximation coincide with the corresponding ones of the classical linear theory for viscoelastic

bodies. In this case, for determination of the values related to the zeroth approximation we use the principle of correspondence by using the Laplace transform

$$\bar{\varphi}(s) = \int_0^\infty \varphi(t)\, e^{-st} dt \tag{17}$$

with the parameter $s > 0$. So, replacing $\sigma_{ij}^{(r_k),0}$, $\varepsilon_{ij}^{(r_k),0}$, $u_i^{(r_k),0}$, $\lambda^{(r_k)}$ and $\mu^{(r_k)}$ in the corresponding equations and relations by $\bar{\sigma}_{ij}^{(r_k),0}$, $\bar{\varepsilon}_{ij}^{(r_k),0}$, $\bar{u}_i^{(r_k),0}$, $\bar{\lambda}^{(r_k)}$ and $\bar{\mu}^{(r_k)}$ respectively, we obtain the field equations, boundary and contact conditions for the Laplace transform of the values of the zeroth approximation. It is evident that, according to the non-homogeneity of the plate material under loading by the bi-axial uniformly distributed normal forces with intensity p_1 and p_3 in the directions of the axes Ox_1 and Ox_3 respectively, that at the ends of the plate the inhomogeneous distributions of the stresses and strains appear in the layers. However, these inhomogeneous distributions arise only in the very near vicinity of the ends of the plate and do not influence the local buckling delamination of the plate parts around the rectangular cracks. Therefore, we do not take the mentioned inhomogeneous distribution of the stresses and strains into account under determination of the Laplace transformation of the values of the zeroth approximation. Thus, using the relations

$$2h_F \bar{\sigma}_{11}^{(2),0}(s) + h_C \bar{\sigma}_{11}^{(1),0}(s) = \frac{1}{s} p_1 h, \quad 2h_F \bar{\sigma}_{33}^{(2),0}(s) + h_C \bar{\sigma}_{33}^{(1),0}(s) = \frac{1}{s} p_3 h,$$

$$\bar{\varepsilon}_{11}^{(1),0}(s) = \bar{\varepsilon}_{11}^{(2),0}(s), \quad \bar{\varepsilon}_{33}^{(1),0}(s) = \bar{\varepsilon}_{33}^{(2),0}(s) \quad \Rightarrow$$

$$\frac{1}{\bar{E}^{*(1)}} \bar{\sigma}_{11}^{(1),0}(s) - \frac{\bar{\nu}^{*(1)}}{\bar{E}^{*(1)}} \bar{\sigma}_{33}^{(1),0}(s) = \frac{1}{\bar{E}^{*(2)}} \bar{\sigma}_{11}^{(2),0}(s) - \frac{\bar{\nu}^{*(2)}}{\bar{E}^{*(2)}} \bar{\sigma}_{33}^{(2),0}(s),$$

$$-\frac{\bar{\nu}^{*(1)}}{\bar{E}^{*(1)}} \bar{\sigma}_{11}^{(1),0}(s) + \frac{1}{\bar{E}^{*(1)}} \bar{\sigma}_{33}^{(1),0}(s) = -\frac{\bar{\nu}^{*(2)}}{\bar{E}^{*(2)}} \bar{\sigma}_{11}^{(2),0}(s) + \frac{1}{\bar{E}^{*(2)}} \bar{\sigma}_{33}^{(2),0}(s) \tag{18}$$

we can write the following expressions for the Laplace transform of the zeroth approximation:

$$\bar{\sigma}_{11}^{(2),0} = \left(\frac{1}{se_1}(p_1 - \bar{\nu}^{*(1)} p_3) + \frac{e_2}{s(e_1)^2}(p_3 - \bar{\nu}^{*(1)} p_1) \right) \left(1 - \frac{(e_2)^2}{(e_1)^2} \right)^{-1},$$

$$\bar{\sigma}_{11}^{(1),0} = \frac{1}{s}(p_1 - \bar{\sigma}_{11}^{(2),0} 2h_F)(h_C)^{-1}$$

$$\bar{\sigma}_{33}^{(2),0} = \frac{1}{s}(p_3 - \bar{\nu}^{(1)} p_1 + e_2 \bar{\sigma}_{11}^{(1),0})(e_1)^{-1}, \quad \bar{\sigma}_{33}^{(1),0} = \frac{1}{s}(p_1 - \bar{\sigma}_{33}^{(2),0} 2h_F)(h_C)^{-1},$$

$$\sigma_{ij}^{(r_k),0} = 0 \text{ for } ij \neq 11;33, \tag{19}$$

where

$$e_1 = 2h_F + h_C \frac{\bar{E}^{*(1)}}{\bar{E}^{*(2)}}, \quad e_2 = 2h_F \bar{\nu}^{*(1)} + \bar{\nu}^{*(2)} h_C \frac{\bar{E}^{*(1)}}{\bar{E}^{*(2)}}. \tag{20}$$

Selecting a suitable expression for the core functions $E^{(r_k)}(t)$ and $\nu^{(r_k)}(t)$ of the integral operators

$$\left\{E^{*(r_k)}; \nu^{*(r_k)}\right\} \phi(t) =$$

$$\left\{E_0^{(r_k)}; \nu_0^{(r_k)}\right\} \phi(t) + \int_0^t \left\{E^{(r_k)}(\beta, t-\tau); \nu^{(r_k)}(\beta, t-\tau)\right\} \phi(\tau) d\tau,$$

and employing some algorithms for calculation of the inverse Laplace transform we can determine the stresses:

$$\sigma_{11}^{(r_k),0} = \sigma_{11}^{(r_k),0}(t), \quad \sigma_{33}^{(r_k),0} = \sigma_{33}^{(r_k),0}(t), \quad \sigma_{ij}^{(r_k),0} = 0 \text{ for } ij \neq 11;33, \tag{21}$$

related to the zeroth approximation.

Now we consider determination of the values of the first approximation. According to the foregoing assumptions (19) and (21) we obtain the following equilibrium equations, mechanical and geometrical relations for the first approximation:

$$\frac{\partial \sigma_{ji}^{(r_k),1}}{\partial x_j} + \sigma_{11}^{(r_k),0}(t) \frac{\partial^2 u_i^{(r_k),1}}{\partial x_1^2} + \sigma_{33}^{(r_k),0}(t) \frac{\partial^2 u_i^{(r_k),1}}{\partial x_3^2} = 0,$$

$$\sigma_{ij}^{(r_k),1} = \lambda^{*(r_k)} \theta^{(r_k),1} \delta_i^j + 2\mu^{*(r_k)} \varepsilon_{ij}^{(r_k),1},$$

$$\varepsilon_{ij}^{(r_k),1} = \frac{1}{2}\left(\frac{\partial u_i^{(r_k),1}}{\partial x_j} + \frac{\partial u_j^{(r_k),1}}{\partial x_i}\right). \tag{22}$$

Consider the boundary and contact conditions obtained for the first approximation:

Boundary conditions at the ends of the plate:

$$u_2^{(r_k),1}\Big|_{x_1=0;\ell_1} = 0, \quad u_2^{(r_k),1}\Big|_{x_3=0;\ell_3} = 0,$$

$$\left[\sigma_{11}^{(r_k),1} + \sigma_{11}^{(r_k),0}(t) \frac{\partial u_1^{(r_k),1}}{\partial x_1}\right]\Bigg|_{x_1=0;\ell_1} = 0, \quad \sigma_{13}^{(r_k),1}\Big|_{x_1=0;\ell_1} = 0,$$

$$\sigma_{31}^{(r_k),1}\Big|_{x_3=0;\ell_3}=0,\qquad \left[\sigma_{33}^{(r_k),1}+\sigma_{33}^{(r_k),0}(t)\frac{\partial u_3^{(r_k),1}}{\partial x_3}\right]\Bigg|_{x_3=0;\ell_3}=0. \tag{23}$$

Boundary conditions on the free face planes of the plate:

$$\sigma_{21}^{(r_1),1}\Big|_{x_2=0}=\sigma_{22}^{(r_1),1}\Big|_{x_2=0}=\sigma_{23}^{(r_1),1}\Big|_{x_2=0}=0,$$

$$\sigma_{21}^{(r_3),1}\Big|_{x_2=h}=\sigma_{22}^{(r_3),1}\Big|_{x_2=h}=\sigma_{23}^{(r_3),1}\Big|_{x_2=h}=0. \tag{24}$$

Boundary conditions on the cracks' edge surfaces:

$$\sigma_{21}^{(r_1),1}\Big|_{\bar{S}_3^-}=\sigma_{11}^{(r_1),0}(t)\frac{\partial f^-}{\partial x_1},\quad \sigma_{22}^{(r_1),1}\Big|_{\bar{S}_3^-}=0,\quad \sigma_{23}^{(r_1),1}\Big|_{\bar{S}_3^-}=\sigma_{33}^{(r_1),0}(t)\frac{\partial f^-}{\partial x_3},$$

$$\sigma_{21}^{(r_2),1}\Big|_{\bar{S}_3^+}=\sigma_{11}^{(r_2),0}(t)\frac{\partial f^+}{\partial x_1},\quad \sigma_{22}^{(r_2),1}\Big|_{\bar{S}_3^+}=0,\quad \sigma_{23}^{(r_2),1}\Big|_{\bar{S}_3^+}=\sigma_{33}^{(r_2),0}(t)\frac{\partial f^+}{\partial x_3},$$

$$\sigma_{21}^{(r_2),1}\Big|_{\bar{S}_4^-}=\sigma_{11}^{(r_2),0}(t)\frac{\partial f^-}{\partial x_1},\quad \sigma_{22}^{(r_2),1}\Big|_{\bar{S}_4^-}=0,\quad \sigma_{23}^{(r_2),1}\Big|_{\bar{S}_4^-}=\sigma_{33}^{(r_2),0}(t)\frac{\partial f^-}{\partial x_3},$$

$$\sigma_{21}^{(r_3),1}\Big|_{\bar{S}_4^+}=\sigma_{11}^{(r_3),0}(t)\frac{\partial f^+}{\partial x_1},\quad \sigma_{22}^{(r_3),1}\Big|_{\bar{S}_4^+}=0,\quad \sigma_{23}^{(r_3),1}\Big|_{\bar{S}_4^+}=\sigma_{33}^{(r_3),0}(t)\frac{\partial f^+}{\partial x_3},$$

$$\bar{S}_3^{\pm}=\{((\ell_1-\ell_{10})/2\le x_1\le(\ell_1+\ell_{10})/2),\\ x_2^{\pm}=h_F\pm 0,\ ((\ell_3-\ell_{30})/2\le x_3\le(\ell_3+\ell_{30})/2)\},$$

$$\bar{S}_4^{\pm}=\{((\ell_1-\ell_{10})/2\le x_1\le(\ell_1+\ell_{10})/2),\\ x_2^{\pm}=h_F+h_C\pm 0,\ ((\ell_3-\ell_{30})/2\le x_3\le(\ell_3+\ell_{30})/2)\}. \tag{25}$$

Contact conditions between the layers of the plate:

$$u_i^{(r_1),1}\Big|_{\wp_1^-}=u_i^{(r_2),1}\Big|_{\wp_1^+},\quad u_i^{(r_3),1}\Big|_{\wp_2^+}=u_i^{(r_2),1}\Big|_{\wp_2^-},$$

$$\sigma_{21}^{(r_1),1}\Big|_{\wp_1^-}=\sigma_{21}^{(r_2),1}\Big|_{\wp_1^+},\quad \sigma_{22}^{(r_1),1}\Big|_{\wp_1^-}=\sigma_{22}^{(r_2),1}\Big|_{\wp_1^+},\quad \sigma_{23}^{(r_1),1}\Big|_{\wp_1^-}=\sigma_{23}^{(r_2),1}\Big|_{\wp_1^+},$$

$$\sigma_{21}^{(r_3),1}\Big|_{\wp_2^+}=\sigma_{21}^{(r_2),1}\Big|_{\wp_2^-},\quad \sigma_{22}^{(r_3),1}\Big|_{\wp_2^+}=\sigma_{22}^{(r_2),1}\Big|_{\wp_2^-},\quad \sigma_{23}^{(r_3),1}\Big|_{\wp_2^+}=\sigma_{23}^{(r_2),1}\Big|_{\wp_2^-}. \tag{26}$$

This completes the formulation of the boundary value problem corresponding to the first approximation.

In a likewise manner the corresponding equations, boundary and contact conditions for the second and subsequent approximations can also be obtained. Thus, investigation of the buckling delamination around an interface rectangular crack contained within a rectangular sandwich plate is reduced to the solutions of series-boundary value problems such as (22)-(26). As in papers by Akbarov and Rzayev (2002a, 2002b, 2003) and others, by direct verification it is proven that the linear equations in (22)-(26) coincide with the corresponding equations for TDLTS presented by Guz (1999).

After determination of the stress-deformation state in the considered plate (using the solution procedure described above) it is necessary to select the stability loss criteria. Similarly to Hoff (1954), for the stability loss criterion we will assume that the case where the size of the initial imperfection starts to increase and grows indefinitely with the external compressive forces (for the elastic plate) or with duration of time (for the viscoelastic plate) under considerable fixed finite values of these forces, is also applicable here. From this criterion, the critical force or the critical time will be determined.

Investigations (which are not detailed here) indicate that the values of the critical force or of the critical time can be determined only within the framework of the zeroth and the first approximations. The second and subsequent approximations do not change the values of the critical parameters. Considering these subsequent approximations improves only the accuracy of the stress distributions in the plate. Since our aim is to investigate the stability loss (i.e. to determine the values of the critical parameters), we restrict ourselves to consideration of the zeroth and first approximations.

According to the foregoing considerations, the stresses in the zeroth approximation have already been determined by the expressions (19)-(21). Now we consider determination of the values of the first approximation for which it is necessary to solve the problem (22)-(26). For this purpose, as for determination of the zeroth approximation, we attempt to use the principle of correspondence by using the Laplace transform (17). It should be noted that under this procedure the following difficulty arises. In the equation (22) and under the conditions (23), $\sigma_{11}^{(r_k),0}(t)$ and $\sigma_{33}^{(r_k),0}(t)$ (as noted above) depend on time and therefore the Laplace transform of the terms $\sigma_{11}^{(r_k),0}(t)\,\partial^2 u_i^{(r_k),1}/\partial x_1^2$ and $\sigma_{33}^{(r_k),0}(t)\,\partial^2 u_i^{(r_k),1}/\partial x_3^2$ in equation (22) and the Laplace transform of the terms $\sigma_{11}^{(r_k),0}(t)\,\partial u_i^{(r_k),1}/\partial x_1$ and $\sigma_{33}^{(r_k),0}(t)\,\partial u_i^{(r_k),1}/\partial x_3$ under the conditions (23) cannot be written as $\bar{\sigma}_{11}^{(r_k),0}\partial^2 \bar{u}_i^{(r_k),1}/\partial x_1^2$, $\bar{\sigma}_{33}^{(r_k),0}\partial^2 \bar{u}_i^{(r_k),1}/\partial x_3^2$, $\bar{\sigma}_{11}^{(r_k),0}\partial \bar{u}_i^{(r_k),1}/\partial x_1$ and $\bar{\sigma}_{33}^{(r_k),0}\partial \bar{u}_i^{(r_k),1}/\partial x_3$, respectively. To

overcome this difficulty we assume that $\sigma_{11}^{(r_k),0}(t)$ and $\sigma_{33}^{(r_k),0}(t)$ vary slowly in time and take the values of $\sigma_{11}^{(r_k),0}(t)$ and $\sigma_{33}^{(r_k),0}(t)$ at some fixed moment $t = t_1$ and consequently, instead of the Laplace transform of the terms $\bar{\sigma}_{11}^{(r_k),0}\partial^2\bar{u}_i^{(r_k),1}/\partial x_1^2$, $\bar{\sigma}_{33}^{(r_k),0}\partial^2\bar{u}_i^{(r_k),1}/\partial x_3^2$, $\bar{\sigma}_{11}^{(r_k),0}\partial\bar{u}_i^{(r_k),1}/\partial x_1$ and $\bar{\sigma}_{33}^{(r_k),0}\partial\bar{u}_i^{(r_k),1}/\partial x_3$ we write $\sigma_{11}^{(r_k),0}(t_1)\partial^2\bar{u}_i^{(r_k),1}/\partial x_1^2$, $\sigma_{33}^{(r_k),0}(t_1)\partial^2\bar{u}_i^{(r_k),1}/\partial x_3^2$, $\sigma_{11}^{(r_k),0}(t_1)\partial\bar{u}_i^{(r_k),1}/\partial x_1$ and $\sigma_{33}^{(r_k),0}(t_1)\partial\bar{u}_i^{(r_k),1}/\partial x_3$, respectively. This assumption, also used in the papers by Rzayev (2002), Rzayev and Akbarov (2002) and Akbarov and Yahnioglu (2001), allows us to obtain accurate results if the variation of $\sigma_{11}^{(r_k),0}$ with respect to time is insignificant. Thus, taking the foregoing discussions into account and replacing $\sigma_{ij}^{(r_k),1}$, $\varepsilon_{ij}^{(r_k),1}$, $u_i^{(r_k),1}$, $\sigma_{11}^{(r_k),0}(t)$, $\lambda^{*(r_k)}$ and $\mu^{*(r_k)}$ in (22)-(26) by $\bar{\sigma}_{ij}^{(r_k),1}$, $\bar{\varepsilon}_{ij}^{(r_k),1}$, $\bar{u}_i^{(r_k),1}$, $\sigma_{11}^{(r_k),0}(t_1)$, $\bar{\lambda}^{*(r_k)}$ and $\bar{\mu}^{*(r_k)}$ respectively, we obtain the corresponding equations and boundary conditions with respect to the Laplace transform of values for the first approximation. For the solution to the problems corresponding to the Laplace transforms of the sought values, we employ the 3D Finite Element Method (3D FEM).

4 FEM modeling of the considered problems

For FEM modeling, when employing the Ritz method, it is necessary to construct the functional, the Euler equation of which the equations (22)-(26) are rewritten for the Laplace transform of the corresponding sought functions. For the realization of this construction the equations (22)-(26) must be self-adjoint ones. In the monograph by Guz (1999) it is proven that the equations of the TDLTS are self-adjoint. According to this statement, we construct the following functional for the problems under consideration:

$$\Pi\left(\bar{u}_1^{(r_k),1},\bar{u}_2^{(r_k),1},\bar{u}_3^{(r_k),1}\right)=$$

$$\sum_{k=1}^{3}\left[\frac{1}{2}\iiint\limits_{V^{(r_k)}}\left[\left(\bar{\sigma}_{11}^{(r_k),1}+\sigma_{11}^{(r_k),0}(t_1)\frac{\partial\bar{u}_1^{(r_k),1}}{\partial x_1}+\sigma_{33}^{(r_k),0}(t_1)\frac{\partial\bar{u}_1^{(r_k),1}}{\partial x_3}\right)\frac{\partial\bar{u}_1^{(r_k),1}}{\partial x_1}+\right.\right.$$

$$\bar{\sigma}_{12}^{(r_k),1}\frac{\partial\bar{u}_1^{(r_k),1}}{\partial x_2}+\bar{\sigma}_{13}^{(r_k),1}\frac{\partial\bar{u}_1^{(r_k),1}}{\partial x_3}+$$

$$\left(\bar{\sigma}_{21}^{(r_k),1}+\sigma_{11}^{(r_k),0}(t_1)\frac{\partial\bar{u}_2^{(r_k),1}}{\partial x_1}+\sigma_{33}^{(r_k),0}(t_1)\frac{\partial\bar{u}_2^{(r_k),1}}{\partial x_3}\right)\frac{\partial\bar{u}_2^{(r_k),1}}{\partial x_1}+$$

$$\bar{\sigma}_{22}^{(r_k),1}\frac{\partial\bar{u}_2^{(r_k),1}}{\partial x_2}+\bar{\sigma}_{23}^{(r_k),1}\frac{\partial\bar{u}_2^{(r_k),1}}{\partial x_3}+$$

$$\left(\bar{\sigma}_{31}^{(r_k),1}+\sigma_{11}^{(r_k),0}(t_1)\frac{\partial \bar{u}_3^{(r_k),1}}{\partial x_1}+\sigma_{33}^{(r_k),0}(t_1)\frac{\partial \bar{u}_3^{(r_k),1}}{\partial x_3}\right)\frac{\partial \bar{u}_3^{(r_k),1}}{\partial x_1}+$$

$$\bar{\sigma}_{32}^{(r_k),1}\frac{\partial \bar{u}_3^{(r_k),1}}{\partial x_2}+\bar{\sigma}_{33}^{(r_k),1}\frac{\partial \bar{u}_3^{(r_k),1}}{\partial x_3}\Bigg]dx_1dx_2dx_3\Bigg]+$$

$$\int_{(\ell_3-\ell_{30})/2}^{(\ell_3+\ell_{30})/2}\int_{(\ell_1-\ell_{10})/2}^{(\ell_1+\ell_{10})/2}\frac{1}{s}\,\sigma_{11}^{(r_1),0}(t_1)\frac{\partial f^-}{\partial x_1}\,\bar{u}_1^{(r_1),1}\Big|_{x_2=h_F-0}dx_1dx_3+$$

$$\int_{(\ell_3-\ell_{30})/2}^{(\ell_3+\ell_{30})/2}\int_{(\ell_1-\ell_{10})/2}^{(\ell_1+\ell_{10})/2}\frac{1}{s}\,\sigma_{33}^{(r_1),0}(t_1)\frac{\partial f^-}{\partial x_3}\bar{u}_3^{(r_1),1}\Big|_{x_2=h_F-0}dx_1dx_3+$$

$$\int_{(\ell_3-\ell_{30})/2}^{(\ell_3+\ell_{30})/2}\int_{(\ell_1-\ell_{10})/2}^{(\ell_1+\ell_{10})/2}\frac{1}{s}\sigma_{11}^{(r_2),0}(t_1)\frac{\partial f^+}{\partial x_1}\bar{u}_1^{(r_2),1}\Big|_{x_2=h_F+0}dx_1dx_3+$$

$$\int_{(\ell_3-\ell_{30})/2}^{(\ell_3+\ell_{30})/2}\int_{(\ell_1-\ell_{10})/2}^{(\ell_1+\ell_{10})/2}\frac{1}{s}\sigma_{33}^{(r_2),0}(t_1)\frac{\partial f^+}{\partial x_3}\bar{u}_3^{(r_2),1}\Big|_{x_2=h_F+0}dx_1dx_3+$$

$$\int_{(\ell_3-\ell_{30})/2}^{(\ell_3+\ell_{30})/2}\int_{(\ell_1-\ell_{10})/2}^{(\ell_1+\ell_{10})/2}\frac{1}{s}\;\sigma_{11}^{(r_2),0}(t_1)\frac{\partial f^-}{\partial x_1}\bar{u}_1^{(r_2),1}\Big|_{x_2=(h_F+h_C)-0}dx_1dx_3+$$

$$\int_{(\ell_3-\ell_{30})/2}^{(\ell_3+\ell_{30})/2}\int_{(\ell_1-\ell_{10})/2}^{(\ell_1+\ell_{10})/2}\frac{1}{s}\;\sigma_{33}^{(r_2),0}(t_1)\frac{\partial f^-}{\partial x_3}\bar{u}_3^{(r_2),1}\Big|_{x_2=(h_F+h_C)-0}dx_1dx_3+$$

$$\int_{(\ell_3-\ell_{30})/2}^{(\ell_3+\ell_{30})/2}\int_{(\ell_1-\ell_{10})/2}^{(\ell_1+\ell_{10})/2}\frac{1}{s}\;\sigma_{11}^{(r_3),0}(t_1)\frac{\partial f^+}{\partial x_1}\bar{u}_1^{(r_3),1}\Big|_{x_2=(h_F+h_C)+0}dx_1dx_3+$$

$$\int_{(\ell_3-\ell_{30})/2}^{(\ell_3+\ell_{30})/2}\int_{(\ell_1-\ell_{10})/2}^{(\ell_1+\ell_{10})/2}\frac{1}{s}\ \sigma_{33}^{(r_3),0}(t_1)\frac{\partial f^+}{\partial x_3}\bar{u}_3^{(r_3),1}\Big|_{x_2=(h_F+h_C)+0}dx_1dx_3. \tag{27}$$

By applying the standard procedure, we obtain the equilibrium equation in (22) and all the boundary and contact conditions (23) – (26) written for stresses from the relation:

$$\delta\Pi=\sum_{k=1}^{3}\left[\frac{\partial\Pi}{\partial\bar{u}_1^{(r_k)}}\,\delta\bar{u}_1^{(r_k)}+\frac{\partial\Pi}{\partial\bar{u}_2^{(r_k)}}\delta\bar{u}_2^{(r_k)}+\frac{\partial\Pi}{\partial\bar{u}_3^{(r_k)}}\delta\bar{u}_3^{(r_k)}\right]=0. \tag{28}$$

Thus, after establishing the foregoing functional by the usual procedure, the FEM technique is applied to obtain the numerical results. In this case, the domain $V\left(=V^{(r_1)}\cup V^{(r_2)}\cup V^{(r_3)}\right)$ is divided into a finite number of finite elements in the form of rectangular prism (brick) elements with eight nodes. The number of finite elements is determined from the convergence requirement of the numerical results. We should note that the authors in the package FTN77 have composed all computer programs used in the numerical investigations carried out.

In the paper by Akbarov, Yahnioglu and Rzayev (2007), it was established that under investigation of the buckling delamination around the cracks contained in a plate, that the numerical results on the critical parameter obtained through the use of singular type finite elements in the vicinity of the crack tips, coincide (with a very high accuracy) with those obtained by the use of ordinary type finite elements in the vicinity of the crack tips. According to this statement, in the present investigation the finite elements containing the crack tips (fronts) are also ordinary brick elements. In this way, we simply establish FEM modeling of the problems under consideration.

Thus, by employing the FEM algorithm detailed above we calculate the values of the Laplace transform of the sought values. The values of the sought functions are determined by the use of the method by Schapery (1966).

5 Numerical results and discussion

The material of the face layers is supposed to be linearly viscoelastic with the operators

$$\begin{aligned}E^{*(2)}&=E_0^{(2)}\left[1-\omega_0R_\alpha^*\left(-\omega_0-\omega_\infty\right)\right],\\ \nu^{*(2)}&=\nu_0^{(2)}\left[1+\frac{1-2\nu_0^{(2)}}{2\nu_0^{(2)}}\omega_0R_\alpha^*\left(-\omega_0-\omega_\infty\right)\right]\end{aligned} \tag{29}$$

where $E_0^{(2)}$ and $\nu_0^{(2)}$ are the instantaneous values of Young's modulus and the Poisson coefficient, respectively; α, ω_0 and ω_∞ are the rheological parameters of the covering layers' materials and R_α^* is the fractional-exponential operator of Rabotnov (1977) and this operator is determined as:

$$R_\alpha^* \varphi(t) = \int_0^t R_\alpha(\beta, t-\tau)\,\varphi(\tau)d\tau \tag{30}$$

where

$$R_\alpha(\beta,t) = t^\alpha \sum_{n=0}^{\infty} \frac{\beta^n t^{n(1+\alpha)}}{\Gamma((1+n)(1+\alpha))}, \quad -1 < \alpha \le 0. \tag{31}$$

In equation (31), $\Gamma(x)$ is the Gamma function.

The material of the core layer is supposed to be pure elastic with mechanical characteristics $E^{(1)}$ (Young's modulus) and $\nu^{(1)}$ (Poisson coefficient).

We introduce the dimensionless rheological parameter $\omega = \omega_\infty/\omega_0$ and the dimensionless time $t' = \omega_0^{1/(1+\alpha)} t$. For concrete numerical investigations, the suitable initial imperfection modes of the crack edge surfaces can be selected as follows:

$$f^{\pm}(x_1,x_3) = \pm \ell_{10} \sin^2\left(\frac{\pi}{\ell_{10}}\left(x_1 - \frac{\ell_1-\ell_{10}}{2}\right)\right) \sin^2\left(\frac{\pi}{\ell_{30}}\left(x_3 - \frac{\ell_3-\ell_{30}}{2}\right)\right),$$

$$(\ell_1-\ell_{10})/2 \le x_1 \le (\ell_1+\ell_{10})/2, \quad (\ell_3-\ell_{30})/2 \le x_3 \le (\ell_3+\ell_{30})/2. \tag{32}$$

Thus, we turn to the analysis of the numerical results and first, we consider the pure elastic stability loss buckling delamination which takes place at $t' = 0$ and $t' = \infty$. We introduce the parameters $\delta_1 = \sigma_{11}^{(1),0}/E^{(1)}$ and $\delta_3 = \sigma_{33}^{(1),0}/E^{(1)}$, and assume that $\delta_3 = \xi\delta_1$. Note that for the fixed value of the parameter ξ we can easily determine the corresponding value of ratio p_3/p_1 from the relations (18) and (19). Moreover, note that through the parameter ξ we estimate the influence of the bi-axiality of the external compression of the plate. Consequently, for each fixed ξ the local buckling delamination of the sandwich plate under consideration can be determined through the critical values of the parameter δ_1.

The critical values of δ_1 obtained at $t' = 0$ and $t' = \infty$ we denote through $\delta_{1cr.0}$ and $\delta_{1cr.\infty}$ respectively. Assume that $h/\ell_1 = 0.15$, $\nu^{(1)} = \nu_0^{(2)} = 0.3$ and $\ell_3/\ell_1 = 1.0$ and consider Table 1 which shows the influence of the parameter ξ on the values of $\delta_{1cr.0}$ (upper number) and $\delta_{1cr.\infty}$ (lower number) obtained for various $E_0^{(2)}/E^{(1)}$ and h_F/ℓ_1 under $\ell_{10}/\ell_1 = 0.5$, $\ell_{30}/\ell_1 = 0.5$ and $\omega = 2$. It follows from this table that, as can be predicted, an increase in the values of ξ causes a decrease in $\delta_{1cr.0}$

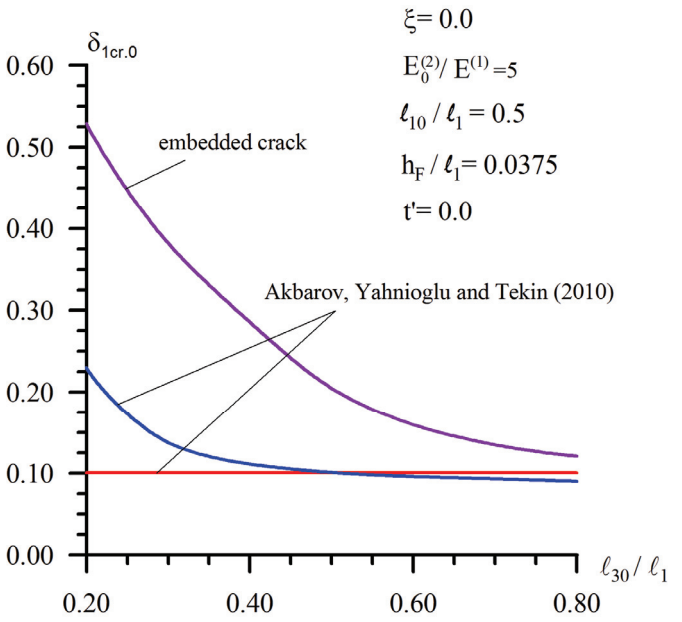

(a)

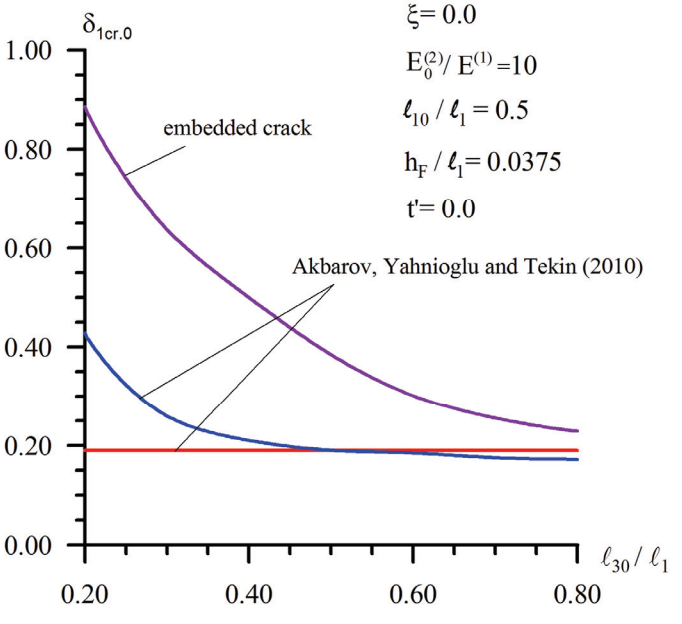

(b)

Figure 2: Comparison of the values of $\delta_{1cr.0}$ obtained for the embedded, edge and band cracks

Table 1: The values of $\delta_{1cr.0}$ (upper number) and $\delta_{1cr.\infty}$ (lower number) obtained for various ξ, $E_0^{(2)}/E^{(1)}$ and h_F/ℓ_1 under $\ell_{30}/\ell_1 = \ell_{10}/\ell_1 = 0.5$

ξ	$E_0^{(2)}/E^{(1)}$	h_F/ℓ_1			
		0.01250	0.02500	0.03750	0.05000
0	1	0.0111 0.0077	0.0251 0.0176	0.0451 0.0317	0.0684 0.0481
	2	0.0220 0.0153	0.0490 0.0346	0.0873 0.0618	0.1322 0.0935
	5	0.0535 0.0374	0.1167 0.0829	0.2051 0.1466	0.3103 0.2213
	10	0.1036 0.0728	0.2215 0.1586	0.3847 0.2773	0.5828 0.4183
0.5	1	0.0077 0.0054	0.0176 0.0124	0.0319 0.0225	0.0488 0.0344
	2	0.0153 0.0107	0.0344 0.0243	0.0618 0.0438	0.0943 0.0668
	5	0.0373 0.0261	0.0819 0.0583	0.1451 0.1038	0.2209 0.1578
	10	0.0722 0.0508	0.1554 0.1114	0.2716 0.1961	0.4135 0.2980
1.0	1	0.0058 0.0040	0.0133 0.0093	0.0241 0.0170	0.0369 0.0260
	2	0.0115 0.0080	0.0260 0.0183	0.0467 0.0331	0.0713 0.0505
	5	0.0281 0.0196	0.0618 0.0440	0.1096 0.0784	0.1671 0.1193
	10	0.0545 0.0383	0.1173 0.0841	0.2052 0.1482	0.3126 0.2254

and $\delta_{1cr.\infty}$. Moreover, this table shows that the values of $\delta_{1cr.0}$ and $\delta_{1cr.\infty}$ also decrease with decreasing $E_0^{(2)}/E^{(1)}$ and h_F/ℓ_1, i.e. with a decrease in the face layer's material stiffness and thickness. These results agree well with the well-known mechanical considerations and give an assurance of the reliability of the developed algorithm and the programs that are used for their calculations. Consider also the following verification of the validity of the developed and used algorithm and programs. For this purpose we use the results obtained under $p_3 = 0$ which, according to the assumption $\nu_0^{(2)} = \nu^{(1)}$, corresponds to the case where $\xi = 0$ and we compare these results with the corresponding ones obtained for the edge and band cracks.

According to the mechanical consideration, for fixed ℓ_{10}/ℓ_1 the values of $\delta_{1cr.0}$ obtained for the above-noted three cases must approach each other with ℓ_{30}/ℓ_1. This consideration is proven with the graphs given in Fig. 2 that show the dependence between $\delta_{1cr.0}$ and ℓ_{30}/ℓ_1 under $\ell_{10}/\ell_1 = 0.5$, $h_F/\ell_1 = 0.0375$, $E_0^{(2)}/E^{(1)} = 5$ (Fig. 2a) and 10 (Fig. 2b). Note that in Fig. 2 the graphs related to the edge and band cracks are taken from the Ref. Akbarov, Yahnioglu and Tekin (2010).

Consider the influence of the cracks' length along the Ox_1 and Ox_3 axes, i.e. the influence of the parameters ℓ_{10}/ℓ_1 and ℓ_{30}/ℓ_1, on the values of $\delta_{1cr.0}$ and $\delta_{1cr.\infty}$. This influence is illustrated by the graphs given in Fig. 3 which are constructed under $\ell_{30}/\ell_1 = 0.5$ and in Fig. 4 which are constructed under $\ell_{10}/\ell_1 = 0.5$. Moreover, under construction of these graphs it is assumed that $\omega = 2$, $h_F/\ell_1 = 0.0375$ and $E_0^{(2)}/E^{(1)} = 2$ (Figs. 3a and 4a), 5 (Figs.3b and 4b) and 10 (Figs. 3c and 4c). It follows from these results that the values of $\delta_{1cr.0}$ and $\delta_{1cr.\infty}$ decrease with ℓ_{10}/ℓ_1 and ℓ_{30}/ℓ_1, but increase with $E_0^{(2)}/E^{(1)}$.

Now we handle the question of how the buckling delamination mode depends on the ratio ℓ_{30}/ℓ_{10}. In this case taking the symmetry of the plate geometry with respect to $x_1 = \ell_1/2$ and with respect to $x_3 = \ell_3/2$, we consider only the parts of the plate for which $V_S = \{0 \le x_1 \le \ell_1/2,\, 0 \le x_3 \le \ell_3/2,\, 0 \le x_2 \le h_F + h_C/2\}$.

Fig. 5 and Fig. 6 show schematically the distribution of $v = u_2^{(2)} E_0^{(2)}/(p_1 \ell_1)$ with respect to $x(= x_1)$ and $z(= \ell_3 - x_3)$ under $x_2 = h_F - 0$ in the cases where $\ell_{30}/\ell_{10} =$ 0.6250, $\ell_{30}/\ell_1 =$0.25, $\xi = 0.5$ (Fig. 5) and $\ell_{30}/\ell_{10} = 0.3571$, $\ell_{30}/\ell_1 =$0.25, $\xi = 0.5$ (Fig. 6) respectively. Under construction of these buckling mode surfaces it is assumed that δ_1 is very near to $\delta_{1cr.0}$, i.e. it is assumed that $|\delta_1 - \delta_{1cr.0}| < 10^{-4}$ is satisfied. Although the illustrated mode surfaces are constructed for the case where $E_0^{(2)}/E^{(1)} = 2$ and $h_F/\ell_1 = 0.0375$ they also hold (in a qualitative sense) for the other values of the problem parameters $E_0^{(2)}/E^{(1)}$ and h_F/ℓ_1. It follows from Fig. 5 that in the case where $\ell_{30}/\ell_{10} = 0.6250$, $\ell_{10}/\ell_1 =$0.40, $\xi = 0.5$ and $\delta_1 =$0.1644 the buckling delamination mode is similar to the initial imperfection mode of the cracks' edge surfaces, but in the case where $\ell_{30}/\ell_{10} = 0.3571$, $\ell_{10}/\ell_1 =$0.70, $\xi =$ 0.5 and $\delta_1 =$0.1458 (Fig. 6) the buckling delamination mode has a more complicate character. For illustration of the influence of the parameters ℓ_{30}/ℓ_{10} and ξ on this character we consider the graphs of the dependence between the values of $w = 2u_2^{(2)} \left| \max\limits_{0 \le x_1 \le \ell_1/2} \left|u_2^{(2)}\right| - \min\limits_{0 \le x_1 \le \ell_1/2} \left|u_2^{(2)}\right| \right|^{-1}$ at $x_2 = h_F - 0$, $x_3 = \ell_3/2$ and x_1/ℓ_1 which are constructed under $h_F/\ell_1 = 0.0375$ and $E_0^{(2)}/E^{(1)} = 2$ for various values of these parameters. These graphs are given in Fig. 7 and in this figure by the letters a, b and c, the cases where $\xi = 0.0$; 0.5 and 1.0 are indicated respectively. It follows

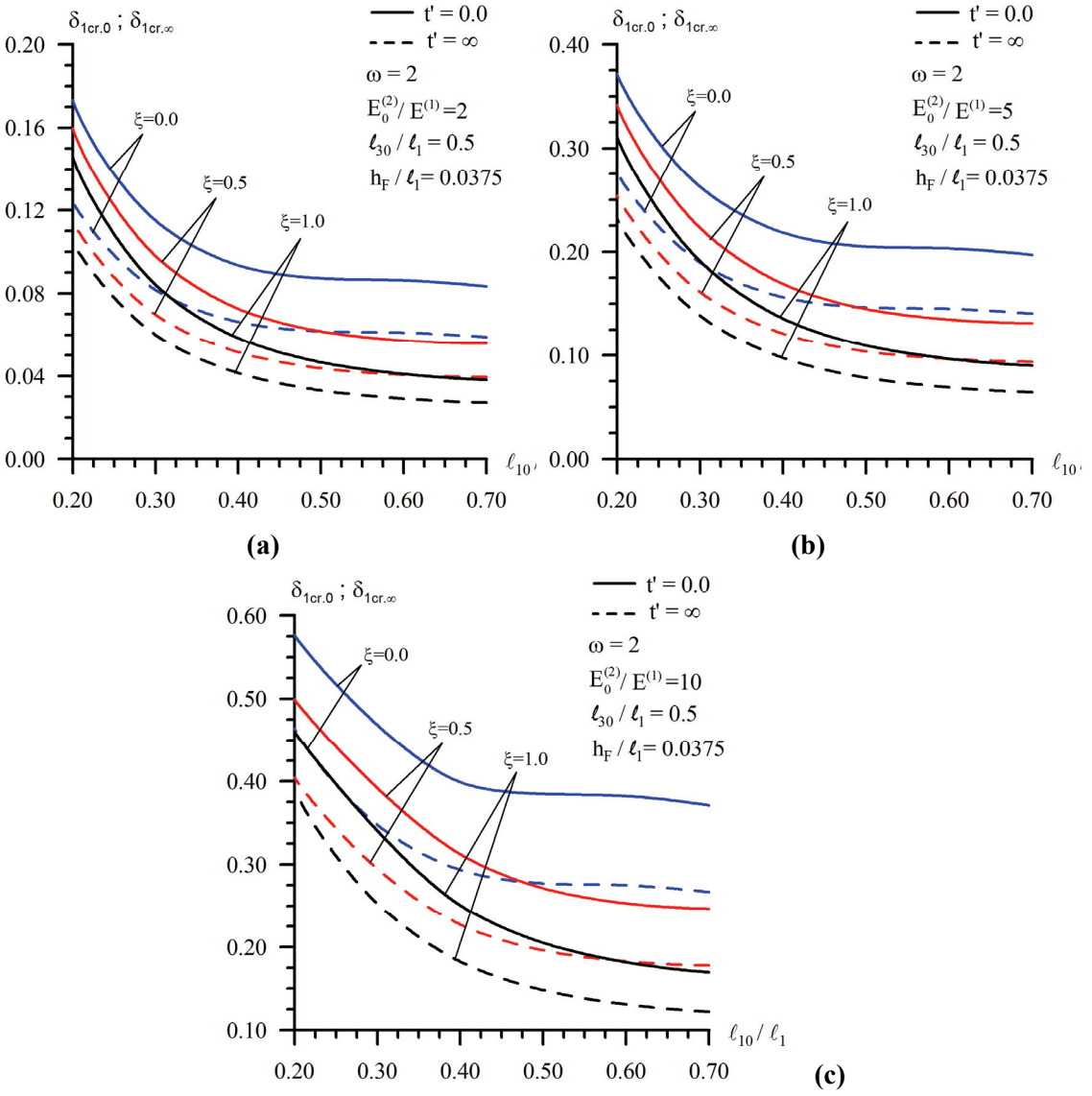

Figure 3: The graphs of the dependencies among $\delta_{1cr.0}$, $\delta_{1cr.\infty}$ and ℓ_{10}/ℓ_1 under $E_0^{(2)}/E^{(1)} = 2$ (a), 5 (b) and 10 (c) under $\omega = 2$, $h_F/\ell_1 = 0.0375$ and $\ell_{30}/\ell_1 = 0.5$

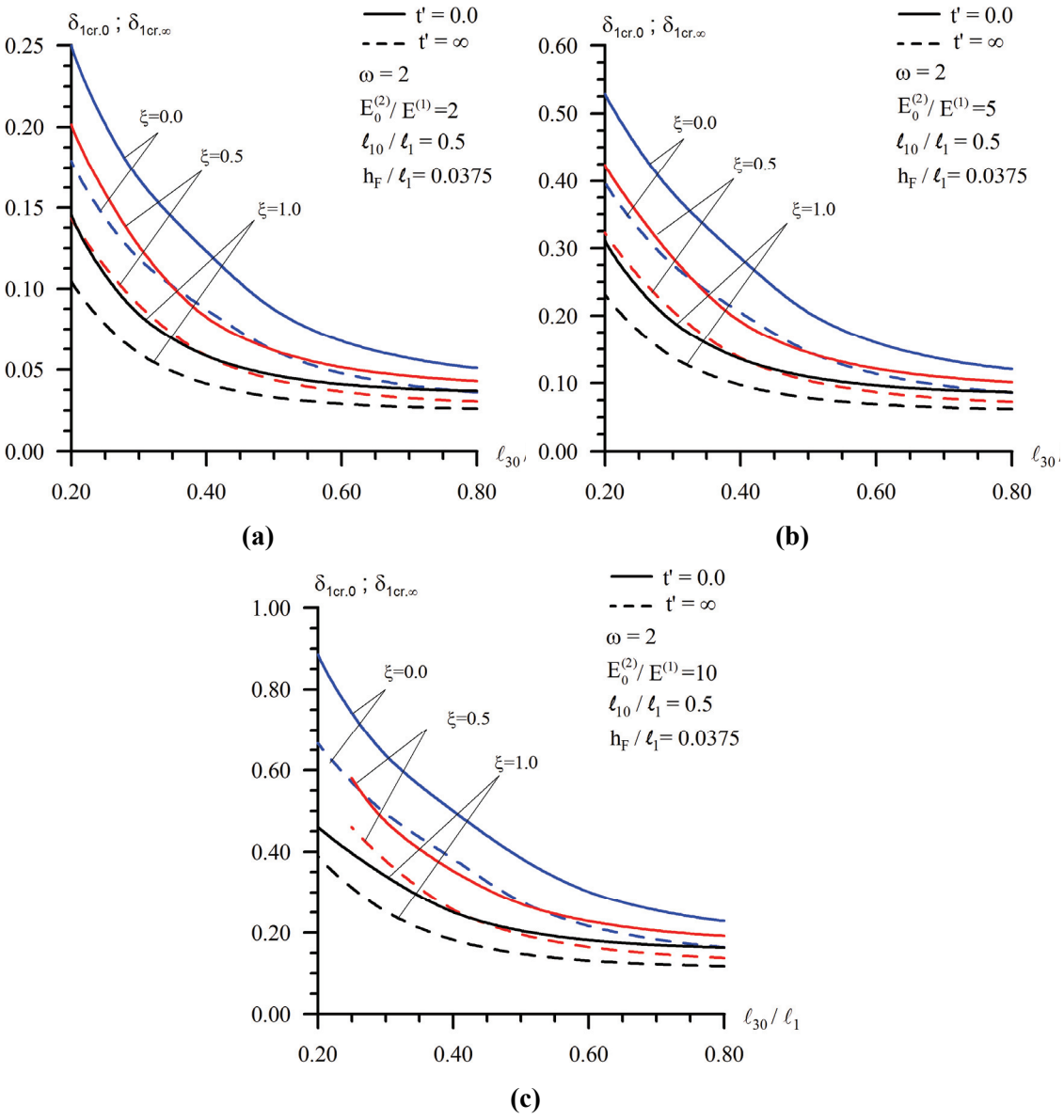

Figure 4: The graphs of the dependencies among $\delta_{1cr.0}$, $\delta_{1cr.\infty}$ and ℓ_{30}/ℓ_1 under $E_0^{(2)}/E^{(1)} = 2$ (a), 5 (b) and 10 (c) under $\omega = 2$, $h_F/\ell_1 = 0.0375$ and $\ell_{10}/\ell_1 = 0.5$

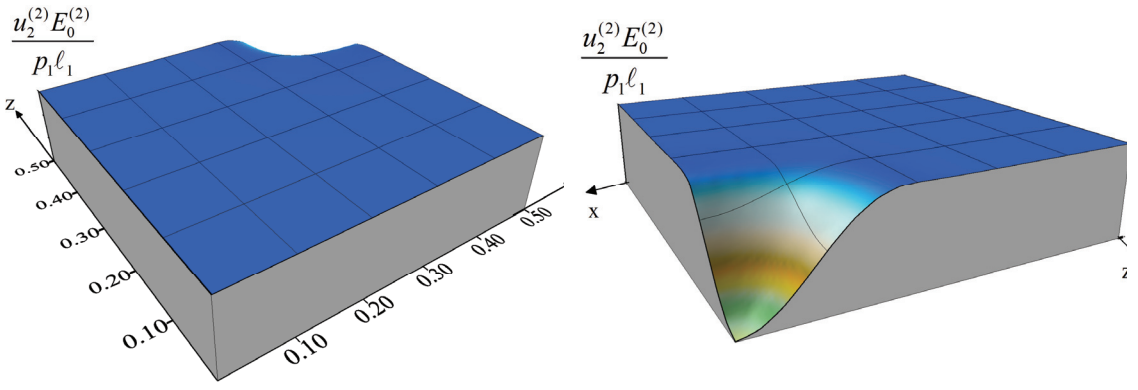

(a) **(b)**

Figure 5: The buckling delamination mode of the crack's edge surface under $t' = 0$, $E_0^{(2)}/E^{(1)} = 2$, h_F/ℓ_1 =0.0375, ℓ_{30}/ℓ_1 =0.25, ℓ_{10}/ℓ_1 =0.40, δ_1 =0.1644: the case where ℓ_{30}/ℓ_{10} =0.6250 and the buckling delamination mode is similar with the initial imperfection mode of the cracks' edges

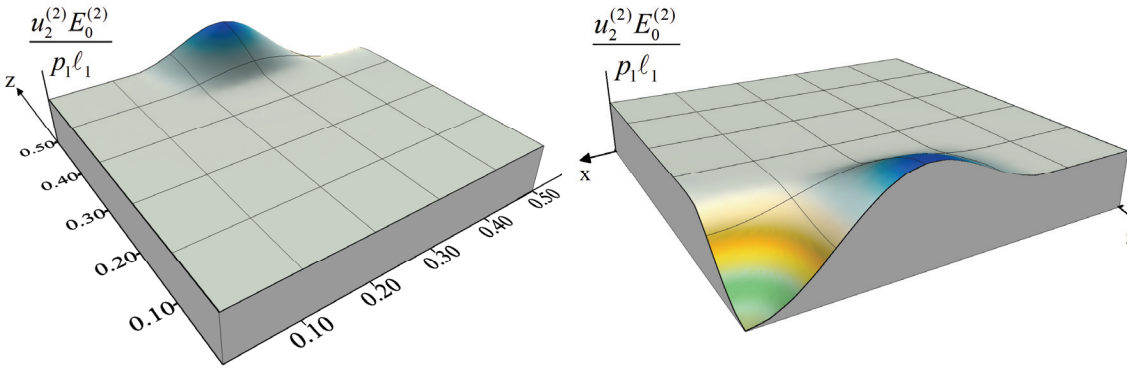

(a) **(b)**

Figure 6: The buckling delamination mode of the crack's edge surface under $t' = 0$, $E_0^{(2)}/E^{(1)} = 2$, h_F/ℓ_1 =0.0375, ℓ_{30}/ℓ_1 =0.25, ℓ_{10}/ℓ_1 =0.70, δ_1 =0.1458: the case where ℓ_{30}/ℓ_{10} =0.3571 and the buckling delamination mode has a complicate character

from the graphs that in general, for fixed values of the problem parameters there exists such values of $\chi\,(=\ell_{30}/\ell_{10})$ (denoted by $\chi*$), according to which the character of the buckling delamination mode can be determined. Thus, for the case considered in Fig. 7, if $\chi > \chi*$, then the buckling delamination mode is similar to the initial imperfection mode, but if $\chi < \chi*$ then the buckling delamination mode is not similar to the initial imperfection mode and has a complicate character. Note that the values of $\chi*$ decrease with the parameter ξ.

It follows from these results that the complicated buckling modes observed in the experimental investigations carried out by Evans and Hutchinson (1995), Gioia and Ortiz (1997), Hutchinson and Suo (1992), Hutchinson, Thouless and Liniger (1992), Nilson and Giannakopoulos (1995), Thouless, Jensen and Liniger (1994), Wang and Evans (1998) and Moon, Chung, Lee, Oh, Wang and Evans, (2002) can be described within the scope of the approach proposed and developed in the present paper.

The violation of the initial imperfection mode of the crack's edges under its evolution with external compressive forces can be explained as follows. In the case considered, the investigation of the evolution of the crack edge-surfaces can be considered approximately as the investigation of the buckling of a "rectangular plate", whose edges are supported elastically. Namely, the "rectangular plate" mentioned above is formed from the part of the plate occupying the region consisting of the part of the face layer, which is between the crack's edge surface and the free face of this layer. During the evolution of the initial imperfection in the ends of this "rectangular plate", various types of stresses and displacements arise. These distributions depend significantly on the ratios ℓ_{30}/ℓ_{10} and h_F/ℓ_1 and determine the buckling mode. Moreover, for clarity of the foregoing discussion, the following known fact in the theory of the stability of rectangular plates should be remembered.

Suppose that the stability loss of the rectangular plate without any initial imperfection with the length ℓ_{10} and the width ℓ_{30} is considered within the scope of the Euler (bifurcation) approach. Furthermore, assume that at the ends of this plate, normal and tangential forces act. As follows from the corresponding theoretical and experimental investigations (see, for example, the monograph by Volmir (1967)), in such cases the stability loss modes of the rectangular plates depend on the ratio of the length to the width.

Now, we consider the numerical results obtained for the critical time, i.e. for t'_{cr}. In obtaining these results, we assume that the values of the strain caused by the external compressive force satisfy the inequality-relation $\delta_{1cr.\infty} < \delta_1 < \delta_{1cr.0}$. We

introduce a parameter:

$$\eta = \frac{\delta_{1cr.0} - \delta_1}{\delta_{1cr.0} - \delta_{1cr.\infty}}. \tag{33}$$

Note that this parameter characterizes the "distance" of the selected value of δ_1 from the values of $\delta_{1cr.0}$ and $\delta_{1cr.\infty}$, and $0 \leq \eta \leq 1$; the values $\eta = 0$ and $\eta = 1$ correspond to the cases where $\delta_1 = \delta_{1cr.0}$ and $\delta_1 = \delta_{1cr.\infty}$, respectively, and for the interval $\delta_{1cr.\infty} < \delta_1 < \delta_{1cr.0}$ the values of η increase (decrease) monotonically with δ_1 approaching $\delta_{1cr.\infty}$ ($\delta_{1cr.0}$). To use the parameter η (33) gives the possibility of determining the influence of the problem parameters (for instance, the parameters $E_0^{(2)}/E^{(1)}$ and ξ) on the critical time (i.e. on t'_{cr}) obtained for the values of δ_1 which have the same "distance" from $\delta_{1cr.0}$ and $\delta_{1cr.\infty}$. Taking the foregoing discussion into account, consider the results given in Tables 2, 3 and 4 which show the values of $t'_{cr.}$ obtained for various η (or δ_1) and $E_0^{(2)}/E^{(1)}$ under $h_F/\ell = 0.0375$, $\ell_{30}/\ell_1 = 0.5$, $\ell_{10}/\ell_1 = 0.5$, $\omega = 2$ and $\alpha = -0.5$ in the cases where $\xi = 0.0$, 0.5 and 1.0 respectively.

Note that under determination of t'_{cr} the values of $\sigma_{11}^{(r_k)}(0)$ and $\sigma_{33}^{(r_k)}(0)$ are taken instead of $\sigma_{11}^{(r_k)}(t)$ and $\sigma_{33}^{(r_k)}(t)$ respectively, which enter the equations (22)-(26).

Thus, it follows from the analyses of the foregoing results that for the fixed value of the parameter η the influence of the parameters $E_0^{(2)}/E^{(1)}$ and ξ is insignificant. Consequently, the parameter on which the values of t'_{cr} depend mainly is η.

Consider the influence of the rheological parameter ω on the values of t'_{cr}. This influence is tabulated in Table 5 under $\alpha = -0.5$, $\xi = 0.0$, $E_0^{(2)}/E^{(1)} = 2$, $h_F/\ell_1 = 0.0375$, $\ell_{30}/\ell_1 = 0.5$ and $\ell_{10}/\ell_1 = 0.5$. Table 5 shows that the values of t'_{cr} increase with ω, because the parameter ω characterizes the dilatational mechanical properties (for instance, the dilatational modulus of elasticity) of the face layers' materials, and an increase in the values of ω means that the stiffness of these materials increases.

Table 6 illustrates the influence of the rheological parameter α on the values of t'_{cr} obtained for the case where $\omega = 2$ under $\xi = 0.0$, $E_0^{(2)}/E^{(1)} = 2$, $h_F/\ell_1 = 0.0375$, $\ell_{30}/\ell_1 = 0.5$ and $\ell_{10}/\ell_1 = 0.5$. It follows from Table 6 that there exists such a value of δ_1 before (after) which an increase in the absolute values of the parameter α causes a decrease (an increase) in the values of the critical time t'_{cr}. Note that these results in the qualitative sense agree with corresponding ones obtained in a paper by Akbarov and Karakaya (2011).

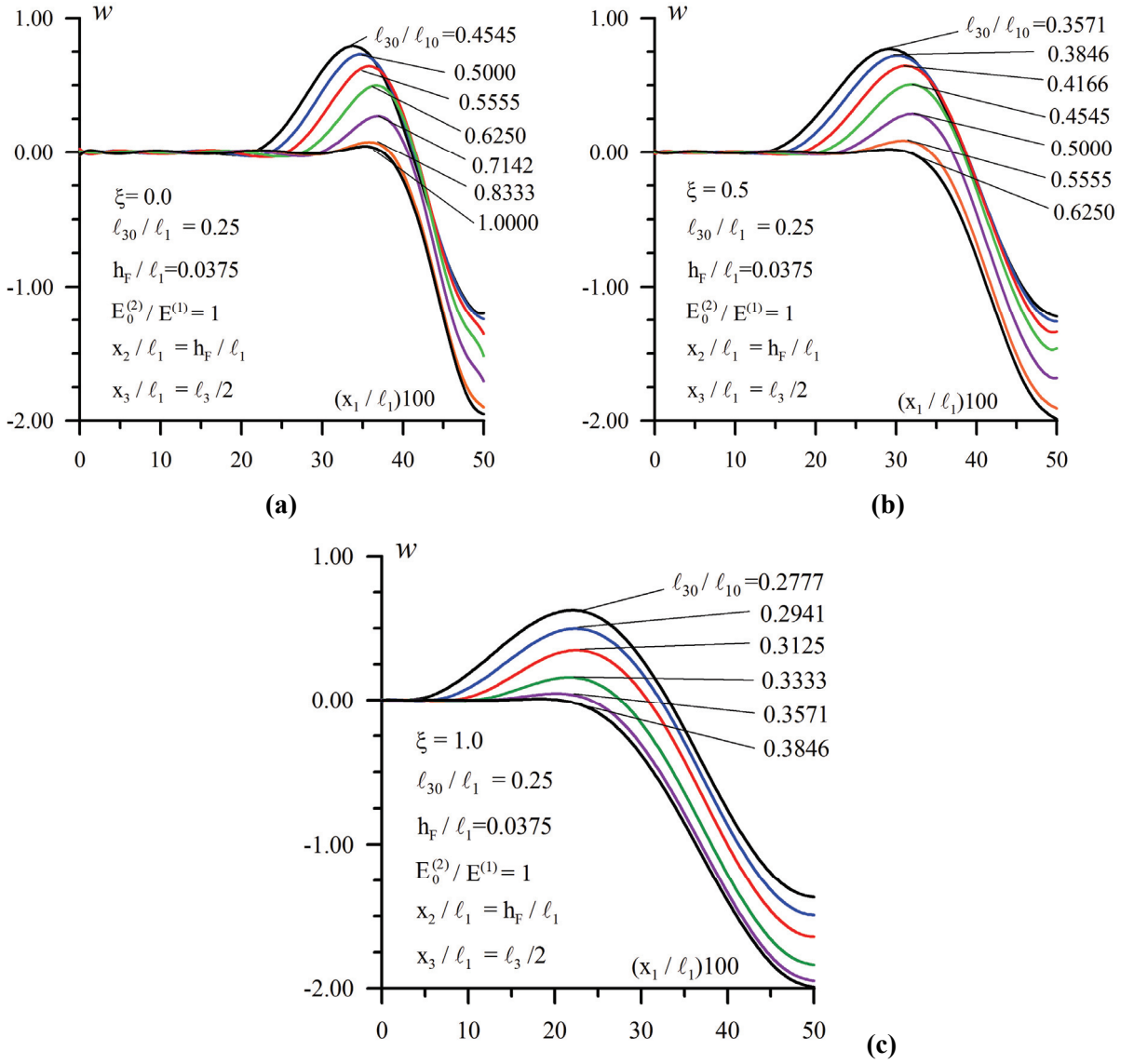

Figure 7: The distribution of the vertical displacement of the cracks' edge surface with respect to x_1/ℓ_1 at $x_3 = \ell_3/2$ in the cases where $\xi = 0$ (a), 0.5 (b) and 1 (c)

Table 2: The values of t'_{cr} obtained for various η and $E_0^{(2)}/E^{(1)}$ under $\xi = 0$ for the case where $\ell_{30}/\ell_1 = \ell_{10}/\ell_1 = 0.5$ and $h_F/\ell_1 = 0.0375$

$E_0^{(2)}/E^{(1)}$	$\delta_{1cr.0}$	$\delta_{1cr.\infty}$	δ_1	η	t'_{cr}
1	0.0451	0.0317	0.043882	0.09	0.0006
			0.041775	0.25	0.006
			0.040633	0.33	0.015
			0.038400	0.50	0.060
			0.036167	0.67	0.244
			0.035050	0.75	0.555
			0.033933	0.83	1.581
			0.033040	0.90	5.370
			0.032918	0.91	6.711
			0.032370	0.95	27.031
2	0.0873	0.0618	0.084982	0.09	0.0006
			0.080973	0.25	0.006
			0.078800	0.33	0.015
			0.074550	0.50	0.060
			0.070300	0.67	0.243
			0.068175	0.75	0.550
			0.066050	0.83	1.550
			0.064350	0.90	5.155
			0.064118	0.91	6.406
			0.063075	0.95	24.527
5	0.2051	0.1466	0.199782	0.09	0.0006
			0.190585	0.25	0.006
			0.185600	0.33	0.015
			0.175850	0.50	0.060
			0.166100	0.67	0.242
			0.161225	0.75	0.547
			0.156350	0.83	1.529
			0.152450	0.90	4.999
			0.151918	0.91	6.185
			0.149525	0.95	22.765

Table 3: The values of t'_{cr} obtained for various η and $E_0^{(2)}/E^{(1)}$ under $\xi = 0.5$ for the case where $\ell_{30}/\ell_1 = \ell_{10}/\ell_1 = 0.5$ and $h_F/\ell_1 = 0.0375$

$E_0^{(2)}/E^{(1)}$	$\delta_{1cr.0}$	$\delta_{1cr.\infty}$	δ_1	η	t'_{cr}
1	0.0319	0.0225	0.031045	0.09	0.0006
			0.029568	0.25	0.006
			0.028767	0.33	0.015
			0.027200	0.50	0.059
			0.025633	0.67	0.240
			0.024850	0.75	0.541
			0.024067	0.83	1.511
			0.023440	0.90	4.949
			0.023355	0.91	6.126
			0.022970	0.95	22.690
2	0.0618	0.0438	0.060164	0.09	0.0006
			0.057334	0.25	0.006
			0.055800	0.33	0.015
			0.052800	0.50	0.060
			0.049800	0.67	0.241
			0.048300	0.75	0.546
			0.046800	0.83	1.533
			0.045600	0.90	5.057
			0.045436	0.91	6.274
			0.044700	0.95	23.559
5	0.1451	0.1038	0.141345	0.09	0.0006
			0.134853	0.25	0.006
			0.131333	0.33	0.015
			0.124450	0.50	0.060
			0.117567	0.67	0.243
			0.114125	0.75	0.550
			0.110683	0.83	1.539
			0.107930	0.90	5.050
			0.107555	0.91	6.252
			0.105865	0.95	23.198

Table 4: The values of t'_{cr} obtained for various η and $E_0^{(2)}/E^{(1)}$ under $\xi = 1$ for the case where $\ell_{30}/\ell_1 = \ell_{10}/\ell_1 = 0.5$ and $h_F/\ell_1 = 0.0375$

$E_0^{(2)}/E^{(1)}$	$\delta_{1cr.0}$	$\delta_{1cr.\infty}$	δ_1	η	t'_{cr}
1	0.0241	0.0170	0.023455	0.09	0.0006
			0.022338	0.25	0.006
			0.021733	0.33	0.015
			0.020550	0.50	0.060
			0.019367	0.67	0.242
			0.018775	0.75	0.547
			0.018183	0.83	1.533
			0.017710	0.90	5.055
			0.017645	0.91	6.278
			0.017355	0.95	23.568
2	0.0467	0.0331	0.045464	0.09	0.0006
			0.043326	0.25	0.006
			0.042167	0.33	0.015
			0.039900	0.50	0.060
			0.037633	0.67	0.242
			0.036500	0.75	0.549
			0.035367	0.83	1.541
			0.034460	0.90	5.102
			0.034336	0.91	6.336
			0.033780	0.95	23.967
5	0.1096	0.0784	0.106764	0.09	0.0006
			0.101859	0.25	0.006
			0.099200	0.33	0.015
			0.094000	0.50	0.061
			0.088800	0.67	0.247
			0.086200	0.75	0.560
			0.083600	0.83	1.576
			0.081520	0.90	5.240
			0.081236	0.91	6.153
			0.079960	0.95	24.913

Table 5: The influence of the rheological parameter ω on the values of t'_{cr} obtained under which $\alpha = -0.5$, $E_0^{(2)}/E^{(1)} = 2$, $h_F/\ell_1 = 0.0375$, $\ell_{30}/\ell_1 = \ell_{10}/\ell_1 = 0.5$ and $\xi = 0$

δ_1	ω		
	0.5	1.0	2.0
0.080973	0.004	0.005	0.006
0.078800	0.009	0.010	0.015
0.074550	0.026	0.033	0.060
0.070300	0.058	0.084	0.243
0.068175	0.083	0.131	0.550
0.066050	0.116	0.203	1.550
0.064350	0.152	0.290	5.155

Table 6: The influence of the rheological parameter α on the values of t'_{cr} obtained under which $\omega = 2$, $E_0^{(2)}/E^{(1)} = 2$, $h_F/\ell_1 = 0.0375$, $\ell_{30}/\ell_1 = \ell_{10}/\ell_1 = 0.5$ and $\xi = 0$

δ_1	α		
	-0.3	-0.5	-0.7
0.080973	0.022	0.006	0.0003
0.078800	0.040	0.015	0.001
0.074550	0.110	0.060	0.014
0.070300	0.298	0.243	0.150
0.068175	0.535	0.550	0.587
0.066050	1.112	1.550	3.296
0.064350	2.646	5.155	24.419

6 Conclusion

In the present paper, an approach was developed and employed for the study of the buckling delamination of elastic and viscoelastic rectangular sandwich plates containing interface rectangular embedded cracks under bi-axial compression. The investigation was made within the scope of the piecewise homogeneous body model. It was assumed that the edge surfaces of the cracks have initial infinitesimal imperfections and the proposed approach was based on the study of the evolution of these initial imperfections with external compressive forces (with duration of time) for pure elastic (viscoelastic) materials. The noted evolution was determined within the scope of the exact 3D geometrically nonlinear field equations of the theory of

elasticity and viscoelasticity. For the solution to the corresponding boundary-value problems, the boundary form perturbation techniques, Laplace transform and 3D FEM were employed. The initial imperfection criterion was used as a delamination buckling (stability loss) criterion. The numerical results on the influence of the problem parameters on the values of the critical strain and critical time as well as on the buckling delamination mode were presented and analyzed. According to these analyses, the following main conclusions can be drawn:

- In unidirectional compression, the values of the critical strains, i.e. the critical values of the parameter δ_1 obtained for the interface rectangular embedded cracks are greater than the corresponding ones obtained for the interface edge and band cracks;

- The bi-axiality of the external compression causes a decrease in the critical values of the parameter δ_1 ;

- The buckling delamination mode of the embedded cracks' edges depends on the value of the ratio ℓ_{30}/ℓ_{10}, where ℓ_{10} (ℓ_{30}) is the crack's length along the Ox_1 (Ox_3) axis;

- The parameter on which the values of the dimensionless critical time mainly depend is the parameter η which characterizes the "distance" of the selected value of the parameter δ_1 from the values of $\delta_{1cr.0}$ and $\delta_{1cr.\infty}$. For a fixed value of the parameter η the influence of the problem parameters $E_0^{(2)}/E^{(1)}$ and ξ on the values of the dimensionless critical time is insignificant;

- With the length of the rectangular embedded crack along the Ox_3 axis the results obtained for the critical values of δ_1 approach the corresponding ones obtained in the paper by Akbarov, Yahnioglu and Tekin (2010) for the edge and band cracks;

- The critical values of the parameter δ_1 increase with the stiffness of the material of the face layers;

- The critical dimensionless time increases with rheological parameter ω, the increasing of which corresponds to an increase in the dilatational modulus of elasticity of the face layers' materials;

- There exists such a value of the parameter δ_1 before (after) which an increase in the absolute values of the rheological parameter α causes an increase (a decrease) in the values of the dimensionless critical time;

- The numerical results obtained and analyzed in the present paper can be taken as a standard for the estimation of the accuracy (in the qualitative and quantitative senses) of the corresponding numerical results obtained within the scope of approximate plate theories.

7 References

Akbarov, S.D. (1998): On the three dimensional stability loss problems of elements of constructions fabricated from the viscoelastic composite materials. *Mech. Comp. Mater*., vol. 34(6), pp. 537-544.

Akbarov, S.D. (2007): Three-dimensional in stability problems for viscoelastic composite materials and structural members. *Inter. Appl. Mech*. 43(10), 1069-1089.

Akbarov, S.D.; Guz, A.N. (2000): *Mechanics of Curved Composites*. Kluwer Academic Publishers, Dordrecht/Boston/London.

Akbarov, S.D.; Karakaya, S. (2011): 3D Analyses of the stability loss of the circular solid cylinder made from viscoelastic composite material. *CMC: Computers, Materials, &Continua*, Vol. 22 (1), pp. 1-38.

Akbarov, S.D.; Rzayev, O.G. (2002a): On the buckling of the elastic and viscoelastic composite circular thick plate with a penny-shaped crack. *Eur. J. Mech. A-Solid,* vol. 21(2), pp. 269-279.

Akbarov, S.D.; Rzayev, O.G. (2002b): Delamination of unidirectional viscoelastic composite materials. *Mech. Comp. Mater*., vol. 38(1), pp. 17-24.

Akbarov, S.D.; Rzayev, O.G. (2003): On the delamination of a viscoelastic composite circular plate. *Inter. Appl. Mech*., vol. 39(3), pp. 368-374.

Akbarov, S.D.; Sisman, T.; Yahnioglu, N. (1997): On the fracture of the unidirectional composites in compression. *Int. J. Eng. Sci*., vol. 35(12/13), pp. 1115-1136.

Akbarov, S.D.; Yahnioglu, N. (2001): The method for investigation of the general theory of stability problems of structural elements fabricated from the viscoelastic composite materials. *Compos. Part B-Eng*., vol. 32(5), pp. 475-482.

Akbarov, S.D.; Yahnioglu, N. (2010): Delamination buckling of a rectangular orthotropic composite plate containing a band crack, *Mechanics of Composite Materials*, vol. 46(5), pp. 493-504.

Akbarov, S.D.; Yahnioglu, N.; Karatas, E.E. (2010): Buckling Delamination of a rectangular plate containing a rectangular Crack and made from elastic and viscoelastic composite materials, *International Journal of Solids and Structures*, vol. 47, pp. 3426-3434.

Akbarov, S.D.; Yahnioglu, N.; Tekin, A. (2010): 3D FEM analyses of the buck-

ling delamination of a rectangular plate containing interface rectangular cracks and made from elastic and viscoelasti materials. *CMES: Computer Modeling in Engineering and Sciences*, Vol. 64 (2), 147–185.

Akbarov, S.D.; Yahnioglu, N.; Rzayev, O.G. (2007): On influence of the singular type finite elements to the critical force in studying the buckling of a circular plate with a crack. *Inter. Appl. Mech*., Vol. 43(9), pp. 120-129.

Bogdanov, V.L.; Guz, A.N.; Nazarenko, V.M. (2009): Fracture of a body with a periodic set of coaxial cracks under forced directed along them: an axisymmetric problem. *Inter. Appl. Mech*., vol. 45(2), pp. 111-124.

Evans, A.G.; Hutchinson, J.W. (1995): The termo mechanical integrity of thin and multilayers. *Acta Metal. Mater.*, vol. 43, pp. 2507-2530.

Gioia, F.; Ortiz, M. (1997): Delamination of compressed thin films. *Adv. Appl. Mech*., vol. 33, pp. 120-192.

Guz, A.N. (1999): *Fundamentals of The Three-Dimensional Theory of Stability of Deformable Bodies*. Springer-Verlag, Berlin Heideberg.

Guz, A.N. (2008a): *Fundamentals of The Compressive Fracture Mechanics of Composites: Fracture in Structure of Materials*, vol. 1. Litera, Kiev (in Russian).

Guz, A.N. (2008b): *Fundamentals of The Compressive Fracture Mechanics of Composites: Related Mechanics of Fracture*, vol. 2. Litera, Kiev (in Russian).

Guz, A.N.; Nazarenko, V. M. (1985a): Theory of near-surface delamination of composite materials under compression along the macro-crack. *Mech. Comp. Mater*., Vol. 21(5), pp. 826-833.

Guz, A. N.; Nazarenko, V. M. (1985b): Symmetric failure of the half-space with penny-shaped crack in compression. *Theor. Appl. Fract. Mech.,* vol. 3, pp. 233-245.

Hoff, N. J. (1954): Buckling and stability. J. Roy. Aeron. Soc. 58(1).

Hutchinson, J.W.; Suo, Z. (1992): Mixed mode cracking in layered materials. *Adv. Appl.Mech*., vol. 29, pp. 63-191.

Hutchinson, J.W.; Thouless, M.D.; Liniger E.G. (1992): Growth and configurational stability of circular, buckling-driven film delaminations. *Acta Metall. Mater*., vol. 40, pp. 295-308.

Moon, M.W.; Chung, J.W.; Lee, K.R.; Oh, K.H.; Wang, R.; Evans, A.G. (2002): An experimental study of the influence of imperfections on the buckling of compressed thin films. *Acta Materialia*, vol. 50, pp. 1219-1227.

Nilsson, K.F.; Giannakopoulos, A.E. (1995): A finite element analysis of configurational stability and finite growth of buckling driven delamination. *J. Mech.*

Phys. Solids, vol. 43, pp. 1983-2021.

Rabotnov, Yu N. (1977): *Elements of Hereditary Mechanics of Solid Bodies*, Nauka, Moskow (in Russian).

Rzayev O.G.; Akbarov S.D. (2002): Local buckling of the elastic and viscoelastic coating around the penny-shaped interface crack. *Int. J. Eng. Sci.,* vol. 40, pp. 1435-1451.

Rzayev O.G. (2002): Local buckling around an interfacial crack in a viscoelastic sandwich plate. *Mechanics of Composite Materials*, vol. 38 (2), pp. 233-242.

Schapery, R.A. (1966): Approximate methods of transform inversion for viscoelastic stress analyses. *Proc. US Nat. Cong. Appl. ASME*, pp. 1075-1085.

Thouless, M.D.; Jensen, H.M.; Liniger, E.G. (1994): Delamination from edge flaws. *Proc. Royal Soc*. London A447, 271-279.

Volmir, A.S. (1967): *Stability of Deformation Systems*, Nauko, Moskow.

Wang, J.S.; Evans, A.G. (1998): Measurement and analysis of buckling and buckle propagation in compressed oxide layers on super ally substrates. *Acta Mater.,* vol.46, pp. 4993-5505.